Since January 2020 Elsevier has created a COVID-19 resource centre with free information in English and Mandarin on the novel coronavirus COVID-19. The COVID-19 resource centre is hosted on Elsevier Connect, the company's public news and information website.

Journal of Colloid and Interface Science 581 (2021) 884–894

Contents lists available at ScienceDirect

Journal of Colloid and Interface Science

journal homepage: www.elsevier.com/locate/jcis

Lip balm drying promotes virus attachment: Characterization of lip balm coatings and XDLVO modeling

Xunhao Wang [a], Reyhan Şengür-Taşdemir [b], İsmail Koyuncu [b,c], Volodymyr V. Tarabara [a,*]

[a] Department of Civil and Environmental Engineering, Michigan State University, East Lansing, MI 48824, USA
[b] National Research Center on Membrane Technologies, Istanbul Technical University, Istanbul, Turkey
[c] Department of Environmental Engineering, Faculty of Civil Engineering, Istanbul Technical University, Istanbul, Turkey

HIGHLIGHTS

- First study of virus adhesion to lipophilic personal care products.
- Coating protocol is developed for studying adhesion to lip balms.
- Drying makes lip balm surface hydrophobic ($G_{sws} < -65$ mJ/m^2) and promotes adhesion.
- XDLVO predicts reversible attachment of viruses to hydrated lip balms.
- Feasibility of QCM-D measurements of virus adhesion to lip balms is demonstrated.

GRAPHICAL ABSTRACT

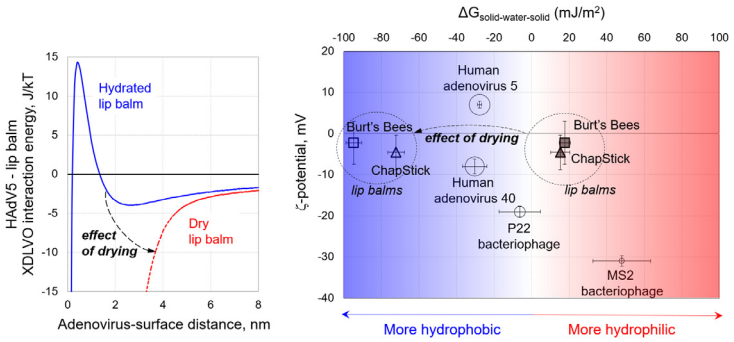

ARTICLE INFO

Article history:
Received 9 June 2020
Revised 29 July 2020
Accepted 29 July 2020
Available online 3 August 2020

Keywords:
Adenovirus
Personal care products
Lip balm
Lipstick
Adhesion
XDLVO
QCM-D
Fomites
Virus transfer
Public health

ABSTRACT

Hypothesis: Drying-induced decrease in lip balm surface energy enhances virus adhesion due to the emergence of strong hydrophobic colloid-surface interactions.

Experiments: A protocol was developed for preparing lip balm coatings to enable physicochemical characterization and adhesion studies. Surface charge and hydrophobicity of four brands of lip balm (dry and hydrated) and human adenovirus 5 (HAdV5) were measured and used to calculate the extended Derjaguin-Landau-Verwey-Overbeek (XDLVO) energy of interactions between lip balm coatings and HAdV5 as well as four other colloids: HAdV40, MS2 and P22 bacteriophages, and SiO_2. Quartz crystal microbalance with dissipation monitoring (QCM-D) tests employed SiO_2 colloids, HAdV5 and hydrated lip balms.

Findings: Drying of lip balms results in a dramatic decrease of their surface energy ($\delta(\Delta G_{sws}) \geq 83.0$ mJ/m^2) making the surfaces highly hydrophobic. For dry lip balms, the interaction of the balm surface with all five colloids is attractive. For lip balms hydrated in 150 mM NaCl (ionic strength of human saliva), XDLVO calculations predict that hydrophilic colloids (MS2, P22, SiO_2) may attach into shallow secondary minima. Due to the relative hydrophobicity of human adenoviruses, primary maxima in XDLVO profiles are low or non-existent making irreversible deposition into primary energy minima possible. Preliminary QCM-D tests with SiO_2 colloids and HAdV5 confirm deposition on hydrated lip balms.

* Corresponding author.
E-mail addresses: wangxunh@msu.edu (X. Wang), rsengur@itu.edu.tr (R. Şengür-Taşdemir), koyuncu@itu.edu.tr (İ. Koyuncu), tarabara@msu.edu (V.V. Tarabara).

https://doi.org/10.1016/j.jcis.2020.07.143
0021-9797/

1. Introduction[1]

Environmental transmission via contaminated surfaces is an important pathway for pathogen transfer that can complement transfer with contaminated food or water, or via direct person-to-person contact. There is a growing body of literature on the pathogen adhesion to and resuspension from fomites [1]. Due to their smaller size, high infectivity, and resistance to disinfection, viruses are of special concern. Despite a clear need for such data, relatively little is known about the propensity of viruses to attach to common surfaces. A number of studies have explored virus transfer to and from human body [2–8]. Most but not all of these studies focused on unmodified human skin Julian et al. [5] showed that washing fingerpads reduced virus transfer; the trend was tentatively attributed to changes in the moisture level or pH of the skin [9] or to the presence of soap residuals pointing to the possible importance of skin coatings. In the two studies by Pitol et al. [6,7], Vaseline was used to delimit the human skin area where bacteriophages were allowed to adhere to human skin. The approach was based on a viability assay, which showed that MS2 adsorption to Vaseline was at least one order of magnitude lower than to the skin. However, the duration of the longest test was 10 min and thus one can assume that Vaseline did not have time to dry.

Microbial contamination of personal care products has been a significant problem for researchers as well as manufacturers worldwide [10]. The presence of high numbers of pathogens poses a serious health threat to consumers, especially those who are already ill or in a weakened state [11]. According to the Rapid Alert System database, from January 2008 until week 26 of 2014 sixty-two cosmetic products were recalled because they were contaminated with pathogenic or potentially pathogenic microorganisms [12]. Although the use of preservatives, good manufacturing practices and quality control programs have improved product quality, cases of contaminated cosmetic products have been reported. For example, on December 7, 2010, there was an Import Alert regarding Alexia Lip gloss cosmetic contaminated by *Sphingomonas paucimobilis* and *P. aeruginosa*, manufactured by Maesa, Jinwan Zhuhai [13]. Legislation and introduction of good manufacturing practices have improved the microbiological standards, but contaminated cosmetics are still found [14] and consequences for end users can be grave. As an example, contaminated ocular cosmetics caused a *Pseudomonas* corneal ulcer after a woman sustained minor corneal trauma with a mascara applicator [15].

Cosmetics are designed and manufactured to ensure product stability and microbiological safety during normal and reasonably foreseeable product use. However, according to the U.S. Food and Drug Administration, personal care products intended for the general population are not intended to be sterile [10]. Personal care products often include natural ingredients, including organic compounds; the raw materials that these natural ingredients are sourced from are one of the main reasons for microbial contamination [16]. Further, cosmetic products can be contaminated during use. Of particular concerns are products such as lipstick and lip balm, which can facilitate contagion through common routes such as ingestion and inhalation. For example, sharing lipstick may increase the chance of infection by Epstein–Barr virus, an agent linked to systemic lupus erythematosus [17]. Lipstick-associated pathogens are most likely to enter the human body through the mouth when eating or drinking. This hypothesized route is of particular importance given the scale of lipstick usage. According to a study conducted by the Scientific Committee on Consumer Safety, the estimated daily amount applied lipstick is 0.057 g and the frequency of application is twice a day [18].

There are multiple studies on virus attachment to surfaces such as organic matter [19], soil [20], membrane filters [21], sand [22], polymers (e.g. polyvinylidene fluoride [23] and anion exchange resins [24]), and polyelectrolyte-coated surfaces [25]. Most of this work employed bacteriophages as human virus surrogates [19,20]. To our knowledge, there has been no published work on the attachment of viruses to personal care products including lip balm and lipsticks. More broadly, to our knowledge, there have been no prior reports on the adhesion of particles of any kind to lip balm or lipstick surfaces. This is likely because of the absence of standard protocols for such measurements and difficulties of sample preparation. The present work aims at filling this knowledge gap.

This study began with developing a methodology for coating lip balms to prepare surfaces suitable for physicochemical characterization of lip balms as well as for testing adhesion of colloids to such materials. Both dry and hydrated lip balms were characterized in terms of charge and hydrophobicity. The data was used to predict the XDLVO energy of interfacial interactions between these surfaces and five colloids: human adenoviruses (serotypes 5 and 40) and two bacteriophages (P22 and MS2), and SiO_2 particles. The XDLVO modeling study was complemented with a preliminary experimental study of SiO_2 and HAdV5 deposition onto hydrated lip balms.

2. Materials and methods

2.1. Reagents

All chemical reagents were of high purity (>99%). Petroleum distillate (Penetrol, PPG Industries) as well as ethyl acetate, isopropanol, methanol, pentane, and hexane (all – Sigma Aldrich) were used as solvents for lip balms. Aqueous solutions of KCl (Sigma Aldrich) were employed in measurements of particle size and electrophoretic mobility of SiO_2 colloids and HAdV5, streaming potential of lip balm surfaces, and colloid adhesion to lip balms. Eight different brands of over-the-counter lip balm, all purchased in the local supermarket (Meijer, Okemos, MI), were initially characterized in water contact angle tests. Based on contact angle values and manufacturer-supplied information on balm composition, four representative types of lip balm were selected for further characterization and colloid adhesion tests. While nanoparticles such as ZnO and TiO_2 are sometimes included in lip balm formulations for added UV protection, neither of the four lip balms selected for this study contained nanoparticles. The detailed composition of each lip balm is given in SM (Table S2). The stock of viable HAdV5 was purchased from American Type Culture Collection (ATCC) [26] (see SM, section S3). As described by the manufacturer, HAdV5 (ATCC VR-1516) was propagated by culturing on HEK 293 cells from the Working Cell Bank in Cell Cubes® and purified using a single-column chromatography with an anion exchange resin. The method was shown to give virus stock of the purity comparable to that achieved with CsCl gradient purification [27]. SiO_2 suspension (Snowtex ZL, 40–41 wt%, , SiO_2 density 2.3 g/cm^3 [28]) was obtained from Nissan Chemical America Corp (Houston, TX).

2.2. Preparation of lip balm surfaces

For contact angle and surface charge measurements, lip balms samples were melted and then spin coated into a relatively thick film on a surface of a glass slide (Protocol A, Fig. 1). Briefly, a solid lip balm sample was first melted on the heater and then pipetted on a glass slide positioned on the chuck of the spin coater operated at 3000 rpm. The deposition procedure was sufficiently fast (~5 s)

[1] Abbreviations: Extended Derjaguin-Landau-Verwey-Overbeek (XDLVO); quartz crystal microbalance with dissipation monitoring (QCM-D); human adenovirus 5 (HAdV5); human adenovirus 40 (HAdV40); American Type Culture Collection (ATCC); scanning electron microscopy (SEM). isoelectric point (IEP).

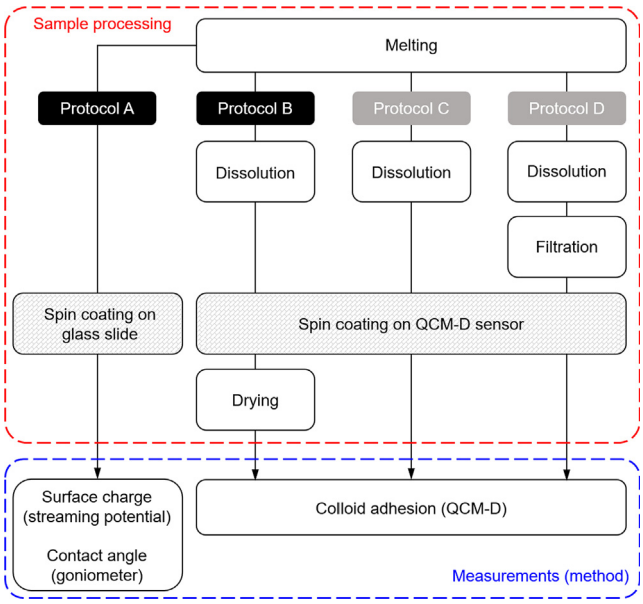

Fig. 1. Lip balm coating protocols evaluated in this work. Of the three protocols (B, C, D) for preparing ultrathin coatings suitable for QCM-D measurements, protocol B yielded lip balm surface with the surface energy most closely matching that of a minimally processed sample (protocol A, baseline) and was, therefore, adopted for studying adhesion of colloids to such coatings.

to avoid premature on-contact solidification of the sample. The duration of spin-coating was 15 s.

For QCM-D measurements, the coating layer should be not only continuous but also very thin (a few microns at most) to avoid overloading the QCM-D sensor. To form such thin layers, melted lip balm samples were mixed with a solvent prior to being spin-coated on the QCM-D sensor surface. First, several solvents - ethyl acetate, isopropanol, methanol, pentane, hexane, and petroleum distillate were evaluated as alternatives for liquefying lip balm. The selection of solvents to test was partly based on the results of a study by Dasari and Goud, who extracted castor seed oil using polar and non-polar solvents [29]. Of the five solvents, petroleum distillate yielded the most homogenous lip balm solution. Then, three different protocols (B, C and D; Fig. 1) were assessed to select a method that gives a sufficiently thin coating with the surface energy most closely matching that of a solvent-free sample. Protocol B gave the best results (see section 3.1). Briefly, solid lip balm samples were melted in a glass vial using a heating plate and then dissolved in petroleum distillate. The liquid sample was stirred (Multistirrer, Thomas Scientific) under 800 rpm and autoreverse (10 s) mode for 1 day and then sonicated overnight at 37 °C to break up larger, undissolved particles. The processed sample (~0.5 ml) was pipetted onto a clean support surface (glass slide or QCM-D sensor), spin-coated at 7500 rpm for 50 s, and left in the fume hood at room temperature for 5 days. After drying, the sample was heated on a heater at the minimum temperature of 100 °C for 2 min to evaporate residual solvents.

2.3. Characterization of the lip balm surface: Surface charge and morphology

Surface charge was determined using streaming current measurements (SurPASS electrokinetic analyzer, Anton Paar GmbH) performed on 20 mm × 10 mm lip balm-coated glass slides. Prior to measurements, each sample was immersed in 1 mM KCl solution overnight. Samples were fixed on sample holders and inserted into an adjustable gap cell with the gap height set at 145 μm. Measurements were done using KCl as the electrolyte and repeated four times for each sample. The homogeneity of the coating on the gold sensors was evaluated using scanning electron microscopy (SEM, JEOL 6610 LV microscope). Because of the concern that volatile components of lip balm samples may interfere with SEM imaging, microscopy was performed in the low vacuum mode (see SM, section S1).

2.4. Characterization of HAdV5 virions and SiO_2 colloids: Size and charge

Hydrodynamic diameter and electrophoretic mobility were measured by dynamic light scattering (ZetaPALS, Brookhaven Instruments) and laser doppler micro-electrophoresis (Zetasizer Nano ZS, Malvern), respectively. Zeta potential values were calculated based on electrophoretic mobilities determined as a function of pH, which was adjusted using NaOH and HCl [30]. The particle size distribution in the SiO_2 stock (40.5 wt%) could not be measured because of high turbidity. Thus, the samples used to measure the particle size and ζ-potential were both diluted to 0.08 wt% in 1 mM KCl. Prior to use, the stock suspensions were sonicated (VWR ultrasonic cleaner, 35 kHz, 40 W, VWR International) for 20 min to ensure complete dispersion. Prior to measuring the hydrodynamic size and charge of colloids (virus or SiO_2), the suspensions were filtered through 0.22 μm filter.

2.5. Quantifying hydrophobicity of HAdV5 and lip balm surfaces

While the hydrophobicity of a surface can be roughly evaluated based on its contact angle with water, a more accurate measure of surface hydrophobicity is given by the free energy of interfacial interaction (ΔG_{sws}) of two surfaces, identical to the one in question, when immersed in water [31]. The negative sign of ΔG_{sws} indicates that the surface is hydrophobic [32]. The absolute value of ΔG_{sws} indicates the degree of hydrophobicity (or hydrophilicity, when $\Delta G_{sws} > 0$) of the surface. To determine ΔG_{sws} for HAdV5 and lip balms (both dry and hydrated), contact angles of three probe liquids - DI water, glycerol, and diiodomethane - on virus lawn and on lip balm surface were determined using the sessile drop method (goniometer/tensiometer model 250, ramé-hart). Contact angle values were calculated by DROPimage Advanced software based on recorded droplets shapes. The droplet volume was in the 8 μl to 10 μl range. To prepare a virus lawn, purified virus stock was filtered through a 50 kDa ultrafiltration membrane. The membrane coated with a multilayer cake of virions (>4 monolayers) was dried until the water contact angle on the membrane stabilized (≥ 6 h across all samples) [21,30,33]. Lip balm surfaces were prepared by spin coating as described in section 2.2. To hydrate lip balm, coated glass slides were immersed for 30 min in NaCl solution with the ionic strength (150 mM) matching that of human saliva. The contact angle tests in air were performed at the ambient temperature of 22 °C and the relative humidity of 47%.

Every contact angle measurement was repeated three times. Surface tension components of the surface (γ_s^{LW}, γ_s^+, γ_s^-) were obtained by substituting measured contact angles and known surface tensions of probe liquids into the Young-Dupré equation (Eq. (1)) where θ is the contact angle of the probe liquid on the surface, γ_l^{TOT} is the total surface energy, while γ^{LW}, $\gamma^+$and γ^- are Lifshitz-van der Waals (i.e. apolar), electron acceptor, and the electron donor components of surface energy. Subscripts l and s refer to the probe liquid and the surface, respectively [31].

$$(1+cos\theta)\gamma_l^{TOT} = 2\left(\sqrt{\gamma_s^{LW}\gamma_l^{LW}} + \sqrt{\gamma_s^+\gamma_l^-} + \sqrt{\gamma_s^-\gamma_l^+}\right) \quad (1)$$

The free energy of interfacial interaction in water, ΔG_{sws}, was calculated (Eq. (2)) based on the surface energy component of the solid (virus or lip balm) and the tabulated values of the surface energy components of water [31]:

$$\Delta G_{sws} = -2\left(\sqrt{\gamma_s^{LW}} - \sqrt{\gamma_w^{LW}}\right)^2 - 4(\sqrt{\gamma_s^+\gamma_s^-} + \sqrt{\gamma_w^+\gamma_w^-} - \sqrt{\gamma_s^+\gamma_w^-} - \sqrt{\gamma_s^+\gamma_w^-} \quad (2)$$

2.6. QCM-D studies of SiO_2 and HAdV5 attachment to lip balm surfaces

Colloidal deposition onto a surface can be quantified using quartz crystal microbalance with dissipation monitoring (QCM-D). This system allows real-time monitoring of the changes in vibrational frequency due to mass deposition onto the quartz crystal sensor. With the deposited mass proportional to the changes in resonance and overtone frequencies, the amount of mass deposited can be computed based on the frequency shift [34]. This technique can also offer information on the viscoelastic behavior of the adsorbed layer by measuring dissipation [35]. QCM-D has been used to study attachment of MS2 bacteriophage [19,20,36], human adenovirus [37] and pathogenic plant viruses [38,39] onto various surfaces such as clays [20], natural organic matter [19,34,40], polyelectrolyte multilayers [25,41], and household paints [37].

The QCM-D E4 system (Biolin Scientific) was used to quantify the deposition of colloids onto the lip balm-coated QCM sensor surfaces. Prior to measurement, gold QCM-D sensors were cleaned following the procedure recommended by the manufacturer (see SM, section S2) and then mounted into the flow chamber to determine their resonance frequency in air. This was followed by a 5-min measurement of resonance frequency to establish a stable baseline. QCM-D tests were carried out at 25 °C in a continuous flow mode (0.15 ml/min) using a digital peristaltic pump (IPC, four channels, ISMATEC). To acquire QCM resonances, lip balm-coated sensors were first contacted with 150 mM NaCl solution for at least 20 min until the baseline of the frequency signals was stabilized using $\frac{\Delta f}{\Delta t} \leq 0.025$ Hz/min as the baseline criterion. The 150 mM solution matched the continuous phase of the colloidal suspension in the QCM-D measurement and had the ionic strength approximating that of human saliva (~136 mM; Table S1) [42]. In tests with SiO_2 colloids, the sensors were challenged with silica suspensions of one of two concentrations: 0.52 mg(SiO_2)/ml or 1.05 mg (SiO_2)/ml. In tests with HAdV5, the concentration of HAdV5 in the feed was ~ 10^9 GC/mL. Based on the measured value of HAdV5 hydrodynamic size (103 nm, see section 3.3) and the approximate virion density (assumed 1.33 g/cm^3 [43,44]) the corresponding mass concentration of HAdV5 was estimated to be 0.76 μg/mL. QCM frequency and dissipation were recorded every 1 min. The frequency shifts were fitted into the Sauerbrey equation [45] to compute the mass change:

$$\Delta m = -C\Delta f/n \quad (3)$$

where C = 17.7 ng·Hz^{-1}·cm^{-2} is the mass sensitivity constant, n is the overtone number and Δf is the frequency shift (Hz). Mass data were calculated based on 3rd and 5th overtones.

2.7. XDLVO modeling of colloid interactions with lip balm

The interactions between particles and surfaces include repulsive electrostatic interactions and attractive van der Waals forces, which can be described by the Derjaguin-Landau-Verwey-Overbeek (DLVO) theory of colloid stability [46,47]. The classic DLVO theory, however, showed only limited ability to predict nanoparticle adhesion to surfaces [19,34,36,48]. Extended DVLO (XDLVO) model [49] builds on the DLVO theory by taking hydrophobic interactions into consideration. The XDLVO theory can predict interactions of dissolved and colloidal materials with various surfaces [50,51] and has been applied to describe virus-surface interactions [21,25,33,52]. The XDLVO theory describes the total energy of interaction $E_{s_1ws_2}^{XDLVO}$ between two surfaces in an aqueous medium as a sum of the Lifshitz-van der Waals, $E_{s_1ws_2}^{LW}$, electrostatic double layer, $E_{s_1ws_2}^{EL}$, an acid-base, $E_{s_1ws_2}^{AB}$, energies. When one of the surfaces is a virus:

$$E_{vws}^{XDLVO} = E_{vws}^{LW} + E_{vws}^{EL} + E_{vws}^{AB} \quad (4)$$

The XDLVO approach extends the DLVO theory by taking hydrophobic interactions ($E_{s_1ws_2}^{AB}$) into consideration. In the expression above,

$$E_{vws}^{LW} = -\frac{Aa}{6d} = 2\pi\frac{a}{d}d_0^2\Delta G_{y0}^{LW} \quad (5)$$

where a is the virus radius, d is the separation distance, d_0 is the minimum separation distance (d_0 = 0.158 nm) [31,53], and $A = -12\pi y_0^2\Delta G_{y0}^{LW}$ is Hamaker constant. Further,

$$E_{vws}^{EL} = \pi\varepsilon_r\varepsilon_0 a\left[2\psi_v\psi_s ln\left(\frac{1+e^{-k_Dd}}{1-e^{-k_Dd}}\right)\right] + (\psi_v^2+\psi_s^2)ln(1-e^{-2k_Dd}) \quad (6)$$

$$E_{vws}^{AB} = 2\pi a\lambda\Delta G_{d_0}^{AB}exp\left(\frac{d_0-d}{\lambda}\right) \quad (7)$$

where ε_r is the dielectric constant of water (ε_r = 79), ε_0 is the relative permittivity in vacuum (ε_0 = 8.854·10^{12}C·V^{-1}·m^{-1}), ψ_v and ψ_s are the surface potentials of the colloid and surface respectively, k_D is the reverse Debye length, λ is the characteristic delay length of the AB interaction (λ = 0.6 nm) [53].

$$\Delta G_{d_0}^{AB} = 2\sqrt{\gamma_s^+}\left(\sqrt{\gamma_s^-} + \sqrt{\gamma_v^-} - \sqrt{\gamma_w^-}\right) + 2\sqrt{\gamma_s^-}\left(\sqrt{\gamma_s^+} + \sqrt{\gamma_v^+} - \sqrt{\gamma_w^+}\right)$$

$$-2(\sqrt{\gamma_s^+\gamma_v^-} + \sqrt{\gamma_s^-\gamma_v^+}) \quad (8)$$

$$\Delta G_{d_0}^{LW} = 2(\sqrt{\gamma_w^{LW}} - \sqrt{\gamma_s^{LW}})(\sqrt{\gamma_v^{LW}} - \sqrt{\gamma_w^{LW}}) \quad (9)$$

where γ^+ is the electron acceptor component, γ^- is the electron donor component and γ^{LW} is the apolar surface energy component. The surface energy components of the surface (γ_s^+, γ_s^-, γ_s^{LW}) and the virus (γ_v^+, γ_v^{LW}, γ_v^-) are calculated using the Young-Dupre equation (Eq. (1)) and contact angle values of the probe liquids.

3. Results and discussion

3.1. Optimal coating protocol and coating morphology

At each processing step, lip balm samples remained homogenous with no apparent changes other than in their flowability. While phase separation may occur in similar materials (e.g. recrystallization of cocoa butter leading to "fat blooms" on the surface of lip balms [54] and chocolate [55]), in our study no phase separation was observed at any point during sample preparation (melting, coating, drying). We attribute this to the relatively simple composition of the lip balms used in this work (see SM, Table S2). Detailed rheological studies would be necessary to explore possible structural and compositional changes in depth [56].

Lip balm film morphology was assessed using SEM (Fig. 2). The coating thickness was relatively constant across the coated area and had a homogeneous internal structure for all lip balms but Vaseline. The thickness was estimated to be 1.15 ± 0.19 μm, 2.03 ± 0.12 μm, 1.07 ± 0.16 μm, and 3.18 ± 0.10 μm for Carmex, ChapStick, Burt's Bees and Vaseline, respectively. The surface

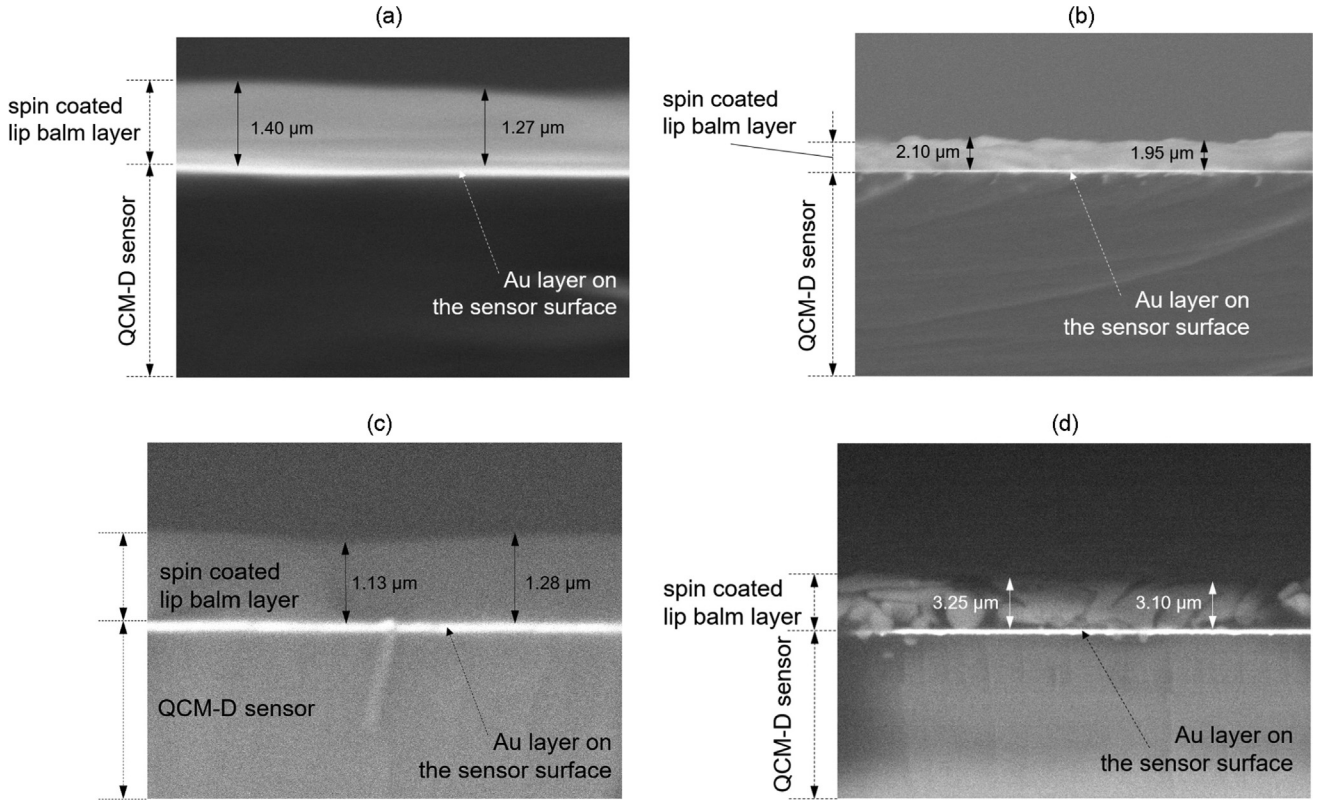

Fig. 2. Representative SEM images of a) Carmex b) ChapStick, c) Burt's Bees, and d) Vaseline coatings on a QCM-D sensor.

roughness of the coatings was not measured more accurately (e.g. with atomic force microscopy). However, how the roughness affected surface energy was captured by the measured values of apparent contact angles. (Surface roughness enhances apparent hydrophobicity of surfaces with water contact angle > 90° [57].) We also note that there may be a difference in the surface roughness (and, therefore, surface energy) between lip balm coatings on a relatively flat surface such as a glass slide, an SEM stub or a QCM-D sensor and that of a human lip. While outside of this study's scope, the effects of the morphology of the underlying surface on the adhesiveness of personal care products should be explored in future work.

Addition of petroleum distillate as a solvent enabled spin-coating of lip balm samples but could also alter the physicochemical properties that affect adhesion. In this study, a change in the surface energy of lip balm was used as a composite indicator of solvent-induced alterations to the sample during the preparation process. The underlying assumption was that the deviation of the surface energy from its baseline value (measured for dry samples) was indicative of the presence of residual solvent. By extension, return of the surface energy value to that of the baseline (protocol A) was accepted as evidence of the removal of residual solvent. The optimal sample preparation procedure was selected in tests with Carmex lip balm coated onto a glass slide surface. Based on measured values of contact angles of probe liquids, surface energies of Carmex coatings made using protocols B, C, and D were compared with that for a coating made using the "solvent-free" protocol A. Protocol B has ΔG_{sws} values matching those obtained by protocol A and, therefore, was selected as the coating method to prepare lip balm surfaces for adhesion studies (Fig. 3).

3.2. Hydrophobicity and surface charge of lip balm-coated surfaces

Lip balms hydrated in 150 mM NaCl (model human saliva) had the surface energy in the 15.2 mJ/m^2 to 38.4 mJ/m^2 range. The energy penalty associated with the replacement of the layer of water molecules bound at such hydrophilic surfaces makes them less adhesive. Drying had a dramatic effect on the surface energy of lip balms (Fig. 4) converting them into strongly hydrophobic surfaces with G_{sws} values ranging from – 65.0 mJ/m^2 to – 90.7 mJ/m^2. Such reversal of the surface energy from positive to highly negative should translate into a significant change in the adhesive properties of these surfaces.

All four lip balms had a pH-dependent charge indicating presence of ionizable surface groups. The ζ-potential of Carmex and Vaseline showed a steady decrease with an increase in pH (Fig. 5a). The isoelectric point (IEP) for Carmex and Vaseline lip balm samples were ~ 4.15 and ~ 4.0, respectively. For ChapStick and Burt's Bees lip balms, the charge had a more complex dependence on pH (Fig. 5b) with two IEPs for each surface: 4.0 and 7.7 for ChapStick and 4.1 and 7.7 for Burt's Bees. The origin of the positive slope in the ζ vs pH dependence for ChapStick and Burt's Bees is unclear. We speculate that this non-monotonous nature of ζ(pH) function is due to the presence of water-soluble compounds in the lip balms with a pH dependent charge and solubility. The observed increase ζ with an increase in pH can stem from leaching of negatively charged compounds at higher pH values. The irregular behavior was observed for only two out of four lip balms and should be explored further. This is particularly important given that the second IPE is close to the pH range of saliva.

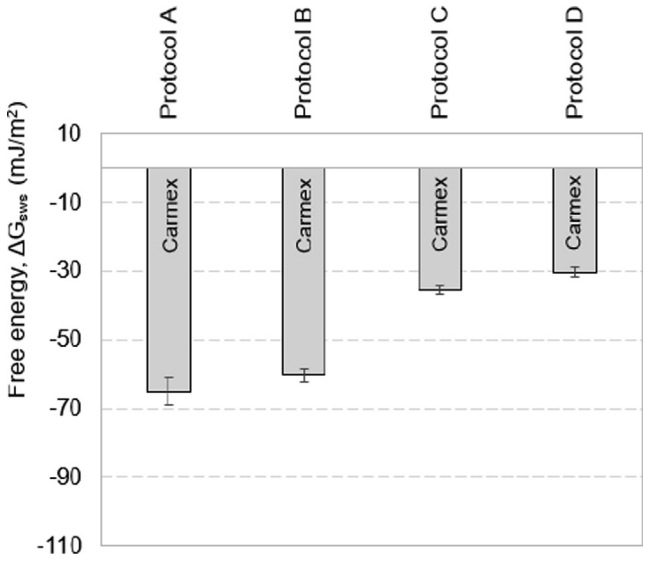

Fig. 3. Free energy of interfacial interaction in water, ΔG_{sws}, of the Carmex lip balm as a function of the coating protocol (see Fig. 1). Measured contact angles of probe liquids and calculated surface energy parameters used to compute ΔG_{sws} values are given in Table S4. Each measurement was done in triplicate. Errors correspond to standard deviations.

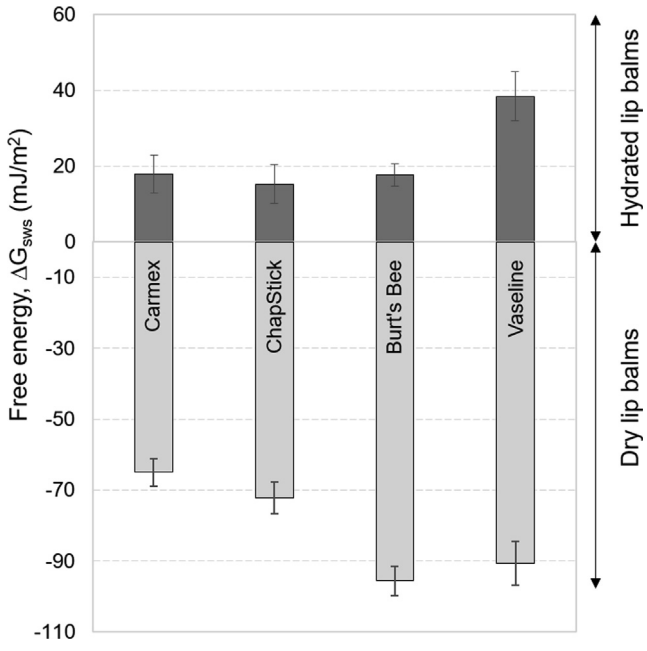

Fig. 4. Free energy of interfacial interaction in water, ΔG_{sws}, of the four lip balms coated using protocol B (see Fig. 1) in dry and hydrated states. Measured contact angles of probe liquids and calculated surface energy parameters used to compute ΔG_{sws} values are given in Table S3. Each measurement was done in triplicate. Errors correspond to standard deviations.

3.3. Hydrodynamic size and surface charge of HAdV5 and SiO_2 colloids

The particle size distribution of HAdV5 suspension had a single narrow peak at ~ 103 ± 1 nm (see SM, Fig. S1) indicating high purity of the stock [26,27]. The ζ-potential of HAdV5 continuously decreases with an increase in pH (Fig. 5). The IEP of HAdV 5 is ~ 4.5 consistent with the result reported by Trilisky and Lenhoff [58]. The ζ-potentials measured at pH < 4.5 and pH > 8 were different from the values reported in that earlier study likely due to differences in the background electrolyte (see SM, section S5).

The particle size distribution of ST-ZL (see SM, Fig. S1) features a single narrow peak at ~ 138 nm, which is above the manufacturer-provided size range (70 to 100 nm). Earlier studies also reported larger sizes for ST-ZL silica (139 to 153 nm [28,59]). The ζ-potential of ST-ZL decreased with an increase in pH (Fig. S4) and remained negative at higher pH values, which is consistent with the result reported by Kim et al. [59]. The ζ-potentials measured at pH < 4 and pH > 8 were different from the result reported by Kim et al. likely due to different background electrolytes used.

3.4. Attachment of viruses and SiO_2 particles to lip balm-coated surfaces: XDLVO predictions

XDLVO modeling of colloid-lip balm interaction was performed for five colloids: two human viruses (HAdV5, HAdV40), two bacteriophages (MS2, P22) and particulate SiO_2. Colloid properties required as inputs to XDLVO model included particle size, ζ-potential and surface energy. For HAdV5, all these characteristics were measured (section 4.3). To our knowledge, this is the first report of surface energy (or any other metric of hydrophobicity) for HAdV5. For SiO_2, size and charge were also determined in this study while the surface energy value was calculated based on contact angles of three probe liquids as reported by Zdziennicka et al. [60]. For HAdV40, P22 and MS2, the values were taken from the literature [21,25,30,60] (Table 1).

Two pH values (4.2 and 7.2) were selected. pH 7.2 represented that of saliva of a healthy person (6.2 to 7.6 typical range [61]). pH 4.2 was chosen to explore HAdV5 deposition under different conditions of virus-balm electrostatic interaction (Fig. 5). In what follows we present results of XDLVO modeling for two colloid/lip balm pairs (SiO_2/Burt's Bees and HAdV5/Carmex). Results for the other colloid/lip balm pairs are given in SM (Fig. S5 – S22).

Fig. 6 shows XDLVO energy profiles for Carmex-HAdV5 interaction. For dry lip balms, the XDLVO model indicates that at both pH values (4.2 and 7.2) the total energy of interaction is attractive: $E_{tot} \leq 0$ and $\frac{dE_{tot}}{dr} \geq 0$ (Fig. 6a, 6c). Fig. 7 illustrates XDLVO energy profiles for Burt's Bees-SiO_2 interaction. For dry balms (Fig. 7a, 7c), the trends were the same as for HAdV5. In fact, for all five colloids and for both pH values, the overall interaction of colloids with *dry* lip balm is always attractive (Fig. S5 – S22). The main reason for the favorable interaction is the high hydrophobicity of dry lip balms (Fig. 4) and the resulting strong short-range hydrophobic attraction.

For *hydrated* lip balms, XDLVO modeling gives a more nuanced prediction. Across the 20 colloid/lip balm combinations evaluated in this work, interaction energy profiles covered a range E_{max} (zero to thousands kT) and E_{min} (zero to ~ 4 kT) values (Table 2; Fig. 6, Fig. 7, Fig. S14-S21). Low E_{max} (<several kT) or no primary energy barrier points to the likely irreversible attachment into the primary minimum. If the primary energy barrier (E_{max}) is high, deposition into the secondary minimum, provided it exists, is possible. Deposition into a secondary minimum is reversible and is stronger (or less reversible) for deeper minima. In the case of SiO_2, hydrating Burt's Bees lip balm flipped its short-range interaction with the colloids from strongly attractive to strongly repulsive (Fig. 7a vs Fig. 7b, Fig. 7c vs Fig. 7d). At the same time, hydration did not have the same dramatic effect on the lip balm's interaction with HAdV5 (Fig. 6a vs Fig. 6b, Fig. 6c vs Fig. 6d). The contrast in the predicted total energy of interaction with hydrated lip balm (attractive interaction with HAdV5 virions versus strongly repulsive interaction with SiO_2 colloids) underscores the importance of the physicochemical properties of the colloids.

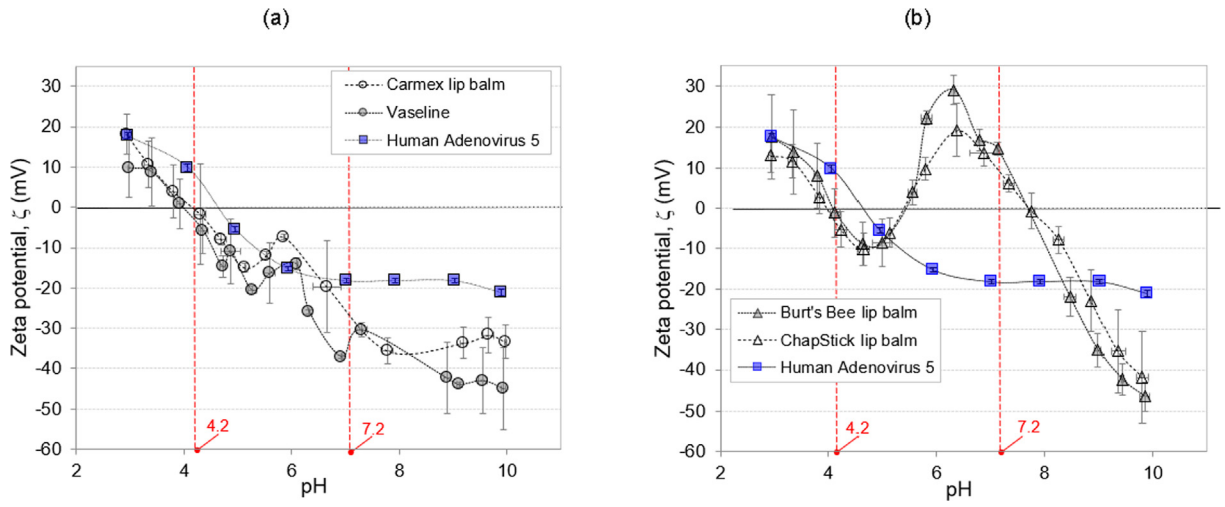

Fig. 5. Surface charge of HAdV5 virions and lip balm surfaces as a function of pH. Vertical dashed lines indicate pH values (4.2 and 7.2) used in QCM-D measurements of HAdV5 attachment to lip balm surfaces. Lines connecting experimental data points are added to the guide the eye. Average and standard deviations for lip balm samples are based on four independent measurements for each lip balm. Average and standard deviations for HAdV5 are based on three independent measurements. HAdV5 data is shown in both graphs to aid data interpretation.

Table 1
Size, charge and hydrophobicity of colloids considered in this work. The three properties are quantified in terms of hydrodynamic diameter (d_h), zeta-potential (ζ) and free energy of interfacial interaction in water (ΔG_{sws}), respectively.

Property	Colloid type				
	SiO_2 particles	Human viruses		Bacteriophages	
		HAdV5	HAdV40	P22	MS2
d_h, nm	137.9 ± 0.4[A] (n = 10)	103 ± 1.3 [A] (n = 10)	98 ± 3.0[B] (n = 10)	54 ± 1.3[C] (n = 10)	27 ± 0.4[C] (n = 10)
ζ, mV (at pH 4.2)	−25 ± 2.9 [G] (n = 10)	7 ± 0.8[H] (n = 30)	−8 ± 1.8[B] (n = 10)	−19 ± 1.3[C] (n = 10)	−31 ± 1.3[C] (n = 10)
ζ, mV (at pH 7.2)	−36 ± 2.8 [G] (n = 10)	−18 ± 0.4[H] (n = 30)	−29 ± 4.7[B] (n = 10)	−47 ± 0.7[C] (n = 10)	−47 ± 0.9[C] (n = 10)
ΔG_{sws}, mJ/m^2	12.8[D]	−27.7 ± 1.1 [E] (n = 3)	−30.4 ± 6.5[B] (n = 3)	−6.3 ± 11.0[C] (n = 3)	48 ± 15.3[F] (n = 3)

Notes: [A]This study (see SM, Fig. S1);[B] Shi et al. [21]; [C] Shi and Tarabara [30]; [D] Calculated based on contact angle data reported by Zdziennicka et al. [60]. The error is not provided because the original contact angle values are reported as averages only; [E] This study (see SM, Table S3); [F] Dang and Tarabara [25]; [G] This study (see SM, Fig. S4); [H] This study (see Fig. 5).

3.5. Attachment of SiO_2 colloids and HAdV5 virions to lip balm-coated surfaces: Preliminary QCM-D study

To our knowledge, there have been no prior studies of particle adhesion to lip balms or other similar lipophilic personal care products. Establishing the experimental methodology for such measurements was one of the goals of this work. To study deposition of viruses in aerosolized droplets onto dry lip balms one would need to work with aerosols and address the number of issues related to the transient processes of droplet evaporation and hydration of the surface upon droplet deposition. The preliminary tests performed in this study were restricted to particle deposition from an aqueous solution onto hydrated lip balms. Longer term QCM-D deposition data were obtained for two colloid/lip balm pairs: SiO_2/Burt's Bees and HAdV5/Carmex.

Silica was selected to avoid any uncertainty related to any other suspended materials possibly present in the feed stock. The conditions of the QCM-D tests with SiO_2/Burt's Bees pair were not conducive to adhesion relative to other pairs (e.g. involving HAdV5 and HAdV40) and could be viewed as a conservative estimate of the extent of particle adhesion to lip balms. The first test was performed using a 1.05 mg(SiO_2)/ml suspension (Fig. 8a). QCM-D frequency data indicated significant deposition (Fig. 8). The monotonous increase in the dissipation signal was consistent with the deposition of colloids onto the lip balm. The total mass of deposited SiO_2 (65 μg) was ~ 0.7% of the mass flown (~9.4 mg) over the lip balm-coated sensor. In early stages of the experiment when the lip balm surface was relatively SiO_2-free, the deposition was determined by SiO_2-lip balm interactions. The surface loading of 74 μg(SiO_2)/cm^2 recorded ~ 1 h into QCM-D test (Fig. 8a) is equivalent to ~ 3 monolayers of colloids. We speculate that this relatively large amount of SiO_2 deposited despite repulsive SiO_2-SiO_2 interactions can be due to the partial "burial" of SiO_2 in the soft hydrated surface of the lip balm. At pH 7.2, SiO_2 and Burt's Bees balm have surface charges of opposite signs (-36 mV and 10 mV, respectively; Fig. 5b) so that electrostatic interactions between these surfaces are favorable. The hydrophobic interactions are strongly repulsive because SiO_2 and hydrated Burt's Bees are both hydrophilic (Table 1, Fig. 4). As a result, XDLVO predicts a very high (>1000 kT) primary barrier and a shallow (~2.6 kT) secondary minimum (Table 3, Fig. 7d). We conclude that SiO_2 deposition occurred into the secondary minimum and should be reversible.

In a companion test (Fig. 8b) on SiO_2 deposition, the lip balm-coated sensor was charged for 30 min with a two-times less concentrated SiO_2 suspension (0.52 mg(SiO_2)/ml) before reverting to the same feed as in test 1 (1.05 mg(SiO_2)/ml). A much weaker deposition was observed throughout the test. At the end of the first stage, the deposit was a submonolayer with the average distance between deposited particles of ~ 0.38 μm (~2 particle diameters). At the end of the long (160 min) second stage, the mass of deposited particles was smaller than in the first test even though the total mass of SiO_2 introduced into the QCM-D chamber in test 2 was higher. The total mass of SiO_2 deposited during test 2

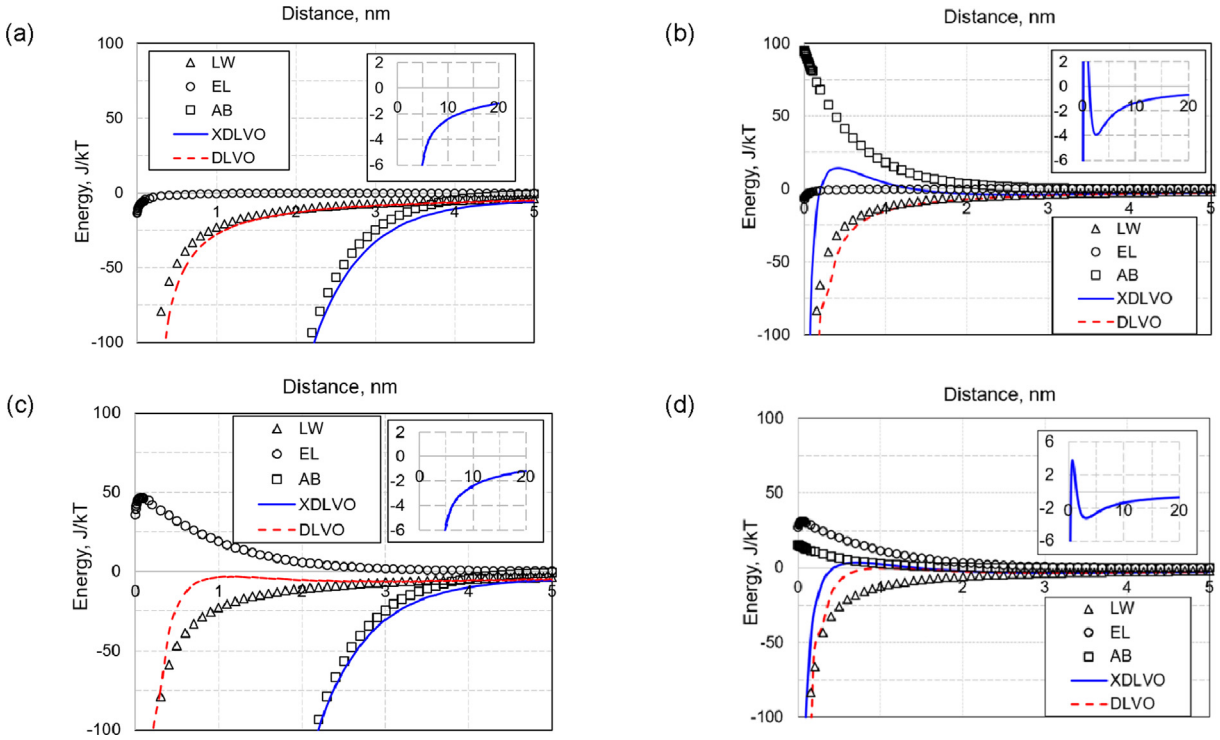

Fig. 6. XDLVO energies of the interaction of human adenovirus 5 with Carmex lip balm at pH 4.2 (a, b) and pH 7.2 (c, d) in dry (a, c) and hydrated (b, d) states. DLVO and XDLVO energy profiles for HAdV5 interaction with the other three lip balms (Burt's Bees, ChapStick and Vaseline) are given in SM. DLVO total energy is provided for reference.

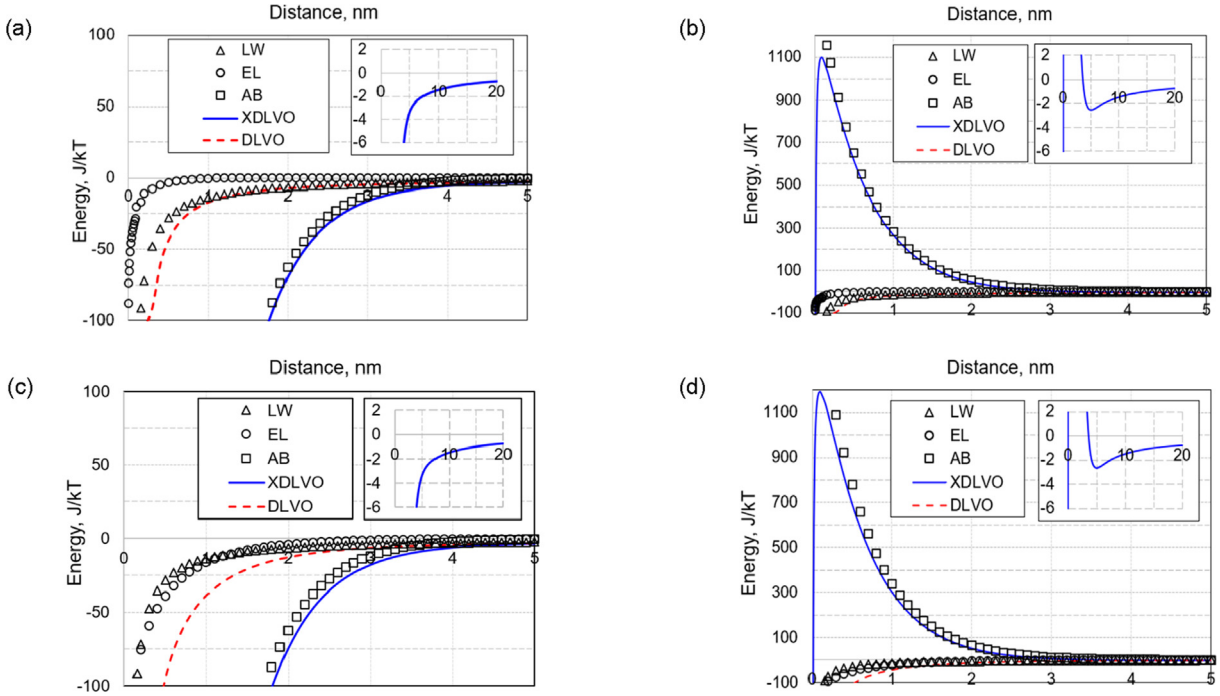

Fig. 7. DLVO and XDLVO energies of the interaction of SiO_2 particles with Burt's Bees lip balm at pH 4.2 (a, b) and pH 7.2 (c, d) in dry (a, c) and hydrated (b, d) states. DLVO and XDLVO energy profiles for HAdV5 interaction with the other three lip balms (Carmex, ChapStick and Vaseline) are given in SM. DLVO total energy is provided for reference.

(38 μg) was ~ 0.14% of the mass flown (27.5 mg) over the lip balm-coated sensor. We conclude that the deposition history is important and that the total mass load of colloids that a lip balm surface is exposed to cannot be a sole predictor of the extent of deposition.

QCM-D tests with HAdV5 were done using as-purchased highly purified stock with HAdV5 concentration of 10^9 GC/mL and Carmex lip balm. Even when undiluted, the mass concentration of HAdV5 stock (~0.76 μg/mL) was ~ 680 times smaller than that of the silica suspension in QCM-D tests with SiO_2. Indeed, a much smaller deposited mass was measured for HAdV5, accompanied by a weaker dissipation signal (Fig. 9). The total mass of deposited HAdV5 (~2.4 μg) was ~ 10.6% of the mass flown (~22.8 μg) over

Table 2
Values (in units of kT) of the primary maximum (E_{max}) and secondary minimum (E_{min}) in the XDLVO energy profile for colloid interaction with hydrated lip balms.

Lip balm (hydrated)	pH	HAdV5		HAdV40		P22		MS2		SiO_2	
		E_{max}	E_{min}	E_{max}	E_{min}	E_{max}	E_{min}	E_{max}	E_{min}	E_{max}	E_{min}
Burt's Bees	4.2	–	–	10.9	−3.1	221.7	−1.1	381.4	−0.5	1099	−2.6
Burt's Bees	7.2	–	–	–	–	158.0	−1.3	378.4	−0.5	1191	−2.6
Carmex	4.2	13.7	−3.9	29.8	−2.9	262.5	−1.2	445.3	−0.5	1448	−2.6
Carmex	7.2	5.2	−3.1	68.6	−2.2	293.0	−1.0	451.0	−0.5	1337	−2.5
ChapStick	4.2	–	–	45.7	−1.9	257.0	−0.8	403.5	−0.4	1192	−1.8
ChapStick	7.2	13.4	−2.8	12.6	−2.3	139.5	−0.9	272.7	−0.4	922	−1.9
Vaseline	4.2	337.7	−2.2	433.3	−1.7	477.0	−0.9	447.0	−0.4	1562	−2.2
Vaseline	7.2	388.0	−2.0	488.0	−1.6	526.0	−0.8	493.0	−0.4	1673	−2.0

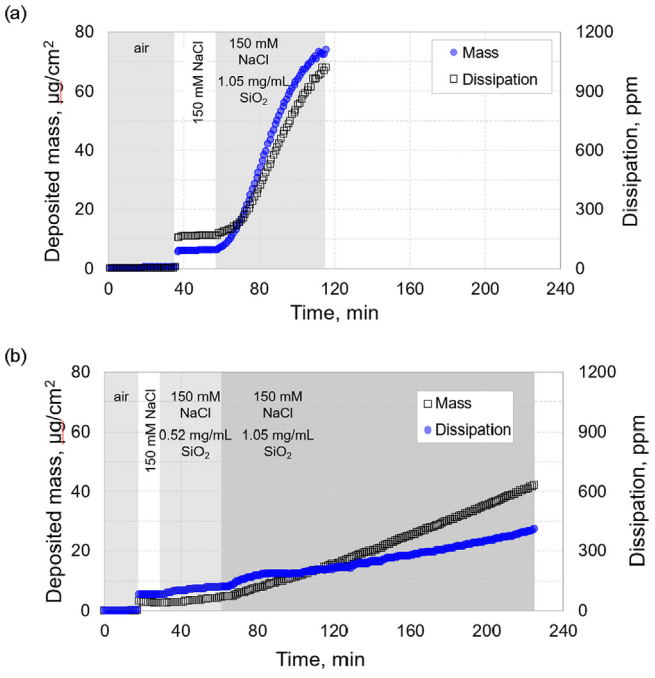

Fig. 8. QCM-D measurements of the deposition of SiO_2 colloids onto hydrated Burt's Bees lip balm under conditions when SiO_2 loading is either a) constant (1.05 mg/ml) or b) increases stepwise from 0.52 mg/ml to 1.05 mg/ml. In both tests, deposition occurs from 150 mM NaCl electrolyte at pH 7.2. The mass values are calculated based on Sauerbrey equation (eq. (3)) with $n = 3$. The results for $n = 5$ are shown in SM (Fig. S23).

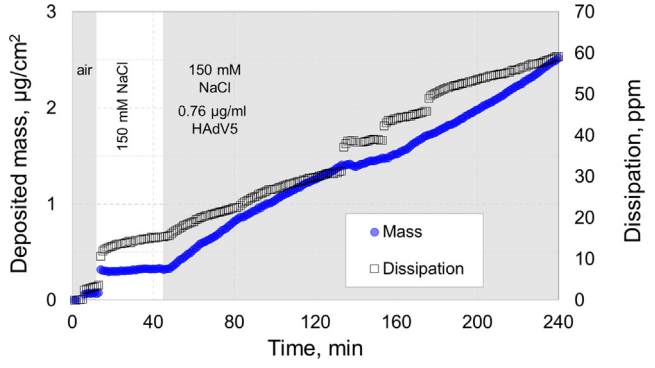

Fig. 9. QCM-D measurements of the deposition of human adenovirus 5 onto hydrated Carmex lip balm from 150 mM NaCl electrolyte at pH 7.2. HAdV5 concentration in the QCM-D feed is ~ 10^9 GC/mL (~0.76 µg/mL). The mass values are calculated based on Sauerbrey equation (eq. (3)) with $n = 3$. The results for $n = 5$ are shown in SM (Fig. S24).

the lip balm-coated sensor. The % deposited value is significantly higher than that for SiO_2 colloids, which is consistent with the much smaller primary energy barrier, E_{max}: 5.2 kT for HAdV5/Carmex versus 1337 kT for SiO_2/Burt's Bees (Table 2). The secondary minimum, E_{min}, was also deeper for HAdV5/Carmex (- 3.1 kT) than for SiO_2/Burt's Bees (- 2.6 kT). We attribute the stronger (relative to the mass loading) deposition of HAdV5 to a more likely association with the lip balms surface through the secondary energy minimum and a possible irreversible attachment into the primary minimum.

Higher mass concentrations in the feed are required for a higher QCM-D signal. To more accurately assess the mass flux towards the sensor surface for a given mass concentration in the feed, one would need to quantify the mass transfer of colloids to the depositional plane. This requires solving the Graetz problem of diffusion-limited transport to a surface from a crossflow [62,63]. In the absence of such solution, the best approach is to employ virus stocks with as high virus titer as possible while still of high purity.

3.6. Implications for virus control and public health protection

The results reported in this work indicate that dry lip balm can serve as a "hot spot" for virus deposition. Given the intended application of lip balms, there is a clear risk to the health of individuals using these products. Low humidity environments (e.g. typical for long air travel) are of particular concern as they promote dehydration. Designing materials to retain surface moisture is one possible approach to staving off adhesion of colloids to lip balms and similar products. A multilayer design with a lipophilic core and a hydrophilic outer layer is one possible strategy.

Likely contagion scenarios should be identified and studied. Possible routes include ingestion of lip balm with associated viruses, ingestion of saliva laden with viruses detached from lip balm, and breathing in viruses resuspended from the lip balm surface into the flow of inhaled air. Given the importance of surface interactions, there is likely a difference between non-enveloped viruses (e.g., adenoviruses, coxsackieviruses, rotavirus) and enveloped viruses (influenza H1N1, human coronaviruses, herpesviruses, hepatitis C) in their propensity to adhere to a lipophilic surface. Future work should explore deposition from other relevant media (e.g. air, respiratory fluid) and onto other surfaces (face and hand creams) as well as virus resuspension into saliva, common drinks (e.g. low pH sodas, milk) and relevant fluid flows (e.g. breathed air).

4. Conclusions

The study reports a protocol for preparing lip balm coatings to enable charge and surface energy measurements as well as adhesion studies with these materials. Surface charge and hydrophobicity were determined for four brands of lip balm. Also measured were size, charge and hydrophobicity of human adenovirus 5. The measured values were used in XDLVO modeling of adenovirus

adhesion to lip balms. Adhesion of four other colloids (HAdV40, MS2 and P22 bacteriophages and SiO_2) spanning a range of sizes, charges and surface energies was also evaluated.

The study tested the hypothesis that a drying-induced increase in lip balm hydrophobicity enhances virus adhesion due to strong hydrophobic colloid-surface interactions. Indeed, drying was shown to result in a dramatic decrease of surface energy ($\delta(\Delta G_{sws}) \geq 83.0$ mJ/m^2) of lip balms making their surfaces highly hydrophobic. XDLVO modelling predicts that attachment to a dry lipstick ($\Delta G_{sws} < -65$ mJ/m^2) is highly favorable as a result of strong short-range hydrophobic attraction. Lip balms hydrated in a solution with the ionic strength of human saliva are hydrophilic ($\Delta G_{sws} > 15$ mJ/m^2) and resist colloid attachment. Physicochemical properties of colloids are also important. Adhesion to lip balms occurs into shallow secondary minima for hydrophilic colloids such as SiO_2, MS2 and P22. Because of the hydrophobicity of adenoviruses, primary maxima in XDLVO profiles are low or non-existent making irreversible deposition into primary minima possible. Preliminary QCM-D tests with SiO_2 colloids and human adenovirus 5 confirm deposition even on a hydrated lip balm.

Prior research focused on virus adhesion to human skin [2–8], or, in two instances [6,7], employed freshly applied Vaseline as a adhesion barrier for MS2. The present work extends these earlier investigations to study virus adhesion to lipophilic personal care products. The proposed methodology can help direct the compositional design of lip balms and similar materials and develop usage guidelines to minimize virus adhesion. Future work should explore deposition from other relevant media (e.g. air, respiratory fluid) and onto other surfaces (e. g. hand creams) as well as virus resuspension into saliva, common drinks (e.g. low pH sodas, milk) and relevant fluid flows (e.g. breathed air).

CRediT authorship contribution statement

Xunhao Wang: Conceptualization, Methodology, Validation, Formal analysis, Investigation, Data curation, Writing - original draft, Writing - review & editing. **Reyhan Şengür-Taşdemir:** Formal analysis, Investigation. **İsmail Koyuncu:** Formal analysis, Resources, Writing - review & editing, Funding acquisition. **Volodymyr V. Tarabara:** Conceptualization, Methodology, Validation, Formal analysis, Investigation, Resources, Data curation, Writing - review & editing, Visualization, Supervision, Project administration, Funding acquisition.

Declaration of Competing Interest

The authors declare that they have no known competing financial interests or personal relationships that could have appeared to influence the work reported in this paper.

Acknowledgements

This material is based upon work supported in part by the National Science Foundation Partnerships for International Research and Education program under Grant IIA-1243433 and in part by the Center for European, Russian and Eurasian Studies at Michigan State University (MSU). We thank Dr. Hang Shi (CTI and Associates, Inc.), Dr. Irene Xagoraraki (Civil and Environmental Engineering, MSU) and Dr. Kristin Parent (Biochemistry and Molecular Biology, MSU) for useful discussions as well as to Dr. Wei Zhang (Department of Plant, Soil and Microbial Sciences, MSU) for providing access to Malvern Zetasizer Nano ZS. We are also thankful to Mrs. Carol Flegler (Center for Advanced Microscopy, MSU) for recording SEM images and advising on appropriate sample preparation procedures.

Appendix A. Supplementary data

Supplementary data to this article can be found online at https://doi.org/10.1016/j.jcis.2020.07.143.

References

[1] B. Stephens, P. Azimi, M.S. Thoemmes, M. Heidarinejad, J.G. Allen, J.A. Gilbert, Microbial exchange via fomites and implications for human health, Curr. Poll. Rep. (2019) 1–16.
[2] S.A. Ansari, S.A. Sattar, V.S. Springthorpe, G.A. Wells, W. Tostowaryk, Rotavirus survival on human hands and transfer of infectious virus to animate and nonporous inanimate surfaces, J. Clin. Microbiol. 26 (8) (1988) 1513–1518.
[3] S.A. Ansari, V.S. Springthorpe, S.A. Sattar, S. Rivard, M. Rahman, Potential role of hands in the spread of respiratory viral infections: Studies with human parainfluenza virus 3 and rhinovirus 14, J. Clin. Microbiol. 29 (10) (1991) 2115–2119.
[4] J.N. Mbithi, V.S. Springthorpe, J.R. Boulet, S.A. Sattar, Survival of hepatitis A virus on human hands and its transfer on contact with animate and inanimate surfaces, J. Clin. Microbiol. 30 (4) (1992) 757–763.
[5] T.R. Julian, J.O. Leckie, A.B. Boehm, Virus transfer between fingerpads and fomites, J. Appl. Microbiol. 109 (6) (2010) 1868–1874.
[6] A.K. Pitol, H.N. Bischel, T. Kohn, T.R. Julian, Virus transfer at the skin–liquid interface, Environ. Sci. Technol. 51 (24) (2017) 14417–14425.
[7] A.K. Pitol, H.N. Bischel, A.B. Boehm, T. Kohn, T.R. Julian, Transfer of enteric viruses adenovirus and coxsackievirus and bacteriophage MS2 from liquid to human skin, Appl. Environ. Microbiol. 84 (22) (2018) e01809–18.
[8] A.M. Wilson, K.A. Reynolds, M.P. Verhougstraete, R.A. Canales, Validation of a stochastic discrete event model predicting virus concentration on nurse hands, Risk Anal. 39 (2019) 1812–1824.
[9] R. Gfatter, P. Hackl, F. Braun, Effects of soap and detergents on skin surface pH, stratum corneum hydration and fat content in infants, Dermatology 195 (1997) 258–262.
[10] S.E. Stewart, M.D. Parker, A. Amézquita, T.L. Pitt, Microbiological risk assessment for personal care products, Int. J. Cosmet. Sci. 38 (6) (2016) 634–645.
[11] L. Jimenez, Microorganisms in the environment and their relevance to pharmaceutical processes, Microbial contamination control in the pharmaceutical industry, CRC Press (2004) 19–32.
[12] E. Neza, M. Centini, Microbiologically contaminated and over-preserved cosmetic products according Rapex 2008–2014, Cosmetics 3 (1) (2016) 3.
[13] M.O. Osungunna, B.B. Oluremi, A. Adetuyi, Bacteriological and antibiotic sensitivity patterns of bacterial isolates from creams and lotions hawked in Sagamu, Ogun State, Pak. J. Nutr. 9 (2010) 773–775.
[14] P.A. Geis, R.T. Hennesy, Preservative development, CRC Press, Florida, 2000, pp. 143–161.
[15] F.R. Reid, T.O. Wood, Pseudomonas corneal ulcer: the causative role of contaminated eye cosmetics, Arch. Ophthalmol. 97 (9) (1979) 1640–1641.
[16] M.D. Lundov, C. Zachariae, Recalls of microbiologically contaminated cosmetics in EU from 2005 to May 2008, Int. J. Cosmetic Sci. 30 (6) (2008) 471–474.
[17] J. Wang, A.B. Kay, J. Fletcher, M.K. Formica, T.E. McAlindon, Is lipstick associated with the development of systemic lupus erythematosus (SLE)?, Clin Rheumatol. 27 (2008) 1183–1187.
[18] The SCCS Notes of Guidance for the Testing of Cosmetic Ingredients and their Safety Evaluation", 9th revision, Scientific Committee on Consumer Safety, SCCS/1564/15, Brussels (2015).
[19] B. Yuan, M. Pham, T.H. Nguyen, Deposition kinetics of bacteriophage MS2 on a silica surface coated with natural organic matter in a radial stagnation point flow cell, Environ. Sci. Technol. 42 (20) (2008) 7628–7633.
[20] M. Tong, Y. Shen, H. Yang, H. Kim, Deposition kinetics of MS2 bacteriophages on clay mineral surfaces, Colloids Surfaces B 92 (2012) 340–347.
[21] H. Shi, I. Xagoraraki, K.N. Parent, M.L. Bruening, V.V. Tarabara, Elution is a critical step for recovering human adenovirus 40 from tap water and surface water by cross-flow ultrafiltration, Appl. Environ. Microbiol. 82 (16) (2016) 4982–4993.
[22] K. Wong, B. Mukherjee, A.M. Kahler, R. Zepp, M. Molina, Influence of inorganic ions on aggregation and adsorption behaviors of human adenovirus, Environ. Sci. Technol. 46 (20) (2012) 11145–11153.
[23] R. Lu, Q. Li, T.H. Nguyen, Random sequential adsorption of human adenovirus 2 onto polyvinylidene fluoride surface influenced by extracellular polymeric substances, J. Colloid Interface Sci. 466 (2016) 120–127.
[24] D.K. Roper, S. Nakra, Adenovirus type 5 intrinsic adsorption rates measured by surface plasmon resonance, Anal. Biochem. 348 (1) (2006) 75–83.
[25] H.T.T. Dang, V.V. Tarabara, Virus deposition onto polyelectrolyte-coated surfaces: A study with bacteriophage MS2, J. Colloid Interface Sci. 540 (2019) 155–166.
[26] Adenovirus Type 5 Reference Material (Product Information Sheet for VR-1516), ATCC, 2020.
[27] B.G. Huyghe, X. Liu, S. Sutjipto, B.J. Sugarman, M.T. Horn, H.M. Shepard, C.J. Scandella, P. Shabram, Purification of a type 5 recombinant adenovirus encoding human p53 by column chromatography, Hum. Gene Ther. 6 (11) (1995) 1403–1416.

[28] C. Boo, S. Lee, M. Elimelech, Z. Meng, S. Hong, Colloidal fouling in forward osmosis: Role of reverse salt diffusion, J. Membr. Sci. 390 (2012) 277–284.
[29] S.R. Dasari, V.V. Goud, Comparative extraction of castor seed oil using polar and non polar solvents, Int. J. Curr. Eng. Technol. 1 (2013) 121–123.
[30] H. Shi, V.V. Tarabara, Charge, size distribution and hydrophobicity of viruses: Effect of propagation and purification methods, J. Virol. Methods 256 (2018) 123–132.
[31] C.J. van Oss, Interfacial forces in aqueous media, CRC Press, 2006.
[32] C.J. van Oss, R.F. Giese, The hydrophilicity and hydrophobicity of clay minerals, Clay Clay Miner. 43 (1995) 474–477.
[33] E.V. Pasco, H. Shi, I. Xagoraraki, S.A. Hashsham, K.N. Parent, M.L. Bruening, V.V. Tarabara, Polyelectrolyte multilayers as anti-adhesive membrane coatings for virus concentration and recovery, J. Membr. Sci. 469 (2014) 140–150.
[34] M. Pham, E.A. Mintz, T.H. Nguyen, Deposition kinetics of bacteriophage MS2 to natural organic matter: Role of divalent cations, J. Colloid Interface Sci. 338 (1) (2009) 1–9.
[35] M.C. Dixon, Quartz crystal microbalance with dissipation monitoring: enabling real-time characterization of biological materials and their interactions, J. Biomol. Tech. 19 (2008) 151–158.
[36] A. Armanious, M. Aeppli, R. Jacak, D. Refardt, T. Sigstam, T. Kohn, M. Sander, Viruses at solid-water interfaces: a systematic assessment of interactions driving adsorption, Environ. Sci. Technol. 50 (2) (2015) 732–743.
[37] H.T.T. Dang, Virus attachment to surfaces: Assessing relative contributions of electrostatic, van der Waals, and acid-base interactions. Ph.D. dissertation, Civil and Environmental Engineering, Michigan State University, 2018.
[38] N.F. Steinmetz, E. Bock, R.P. Richter, J.P. Spatz, G.P. Lomonossoff, D.J. Evans, Assembly of multilayer arrays of viral nanoparticles via biospecific recognition: a quartz crystal microbalance with dissipation monitoring study, Biomacromol. 9 (2) (2008) 456–462.
[39] X. Huang, J. Xu, H.-F. Ji, G. Li, H. Chen, Quartz crystal microbalance based biosensor for rapid and sensitive detection of maize chlorotic mottle virus, Anal. Method. 6 (13) (2014) 4530–4536.
[40] L. Gutierrez, S.E. Mylon, B. Nash, T.H. Nguyen, Deposition and aggregation kinetics of rotavirus in divalent cation solutions, Environ. Sci. Technol. 44 (12) (2010) 4552–4557.
[41] G. Tiliket, G. Ladam, Q.T. Nguyen, L. Lebrun, Polyethylenimine surface layer for enhanced virus immobilization on cellulose, Appl. Surf. Sci. 370 (2016) 193–200.
[42] G. Ross, Essentials of human physiology, Yearbook Medical Publishers Chicago (1978).
[43] G.W. Gary, J.C. Hierholzer, R.E. Black, Characteristics of noncultivable adenoviruses associated with diarrhea in infants: a new subgroup of human adenoviruses, J. Clin. Microbiol. 10 (1) (1979) 96–103.
[44] G. Winberg, G. Wadell, Structural polypeptides of adenovirus type 16 incomplete particles, J. Virol. 22 (2) (1977) 389–401.
[45] G. Sauerbrey, Verwendung von Schwingquarzen zur Wägung dünner Schichten und zur Mikrowägung, Zeitschrift für physik 155 (2) (1959) 206–222.
[46] B. Derjaguin, L. Landau, Theory of the stability of strongly charged lyophobic sols and of the adhesion of strongly charged particles in solutions of electrolytes, Acta Physico Chimica URSS 14 (1941) 633–662.
[47] E.J.W. Verwey, J. Th G. Overbeek, Theory of the stability of lyophobic colloids, Elsevier, Amsterdam, 1948.
[48] C. Dika, M.H. Ly-Chatain, G. Francius, J.F.L. Duval, C. Gantzer, Non-DLVO adhesion of F-specific RNA bacteriophages to abiotic surfaces: importance of surface roughness, hydrophobic and electrostatic interactions, Colloids Surfaces A 435 (2013) 178–187.
[49] C.J. van Oss, M.K. Chaudhury, R.J. Good, Interfacial Lifshitz-van der Waals and polar interactions in macroscopic systems, Chem. Rev. 88 (1988) 927–941.
[50] Y. Chen, L. Shen, R. Li, X. Xu, H. Hong, H. Lin, J. Chen, Quantification of interfacial energies associated with membrane fouling in a membrane bioreactor by using BP and GRNN artificial neural networks, J. Colloid Interface Sci. 565 (2020) 1–10.
[51] J. Teng, L. Shen, Y. Xu, Y. Chen, X.-L. Wu, Y. He, J. Chen, H. Lin, Effects of molecular weight distribution of soluble microbial products (SMPs) on membrane fouling in a membrane bioreactor (MBR): Novel mechanistic insights, Chemosphere 248 (2020) 126013.
[52] Y. Xing, A. Ellis, M. Magnuson, W.F. Harper, Adsorption of bacteriophage MS2 to colloids: Kinetics and particle interactions, Colloids Surfaces A 585 (2020) 124099.
[53] J.A. Brant, A.E. Childress, Assessing short-range membrane–colloid interactions using surface energetics, J. Membr. Sci. 203 (1–2) (2002) 257–273.
[54] A.R. Fernandes, M.F. Dario, C.A.S. de Oliveira Pinto, T.M. Kaneko, A.R. Baby, M.V. R. Velasco, Stability evaluation of organic lip balm, Braz. J. Pharmaceut. Sci. 49 (2013) 293–299.
[55] I. Foubert, I.V. Cauteren, K. Dewettinck, A. Huyghebaert, Differential scanning calorimetry as a means of predicting chocolate fat-blooming, in: N. Widlak, R. Hartel, S. Narine (Eds.), Crystallization and solidification properties of lipids, AOCS Press, 2001, pp. 79–86.
[56] S. Pan, N. Germann, Mechanical response of industrial benchmark lipsticks under large-scale deformations, Acta Mechanica 231 (2020) 3031–3042.
[57] A.W. Adamson, A.P. Gast, Physical Chemistry of Surfaces, Wiley - Interscience (1997).
[58] E.I. Trilisky, A.M. Lenhoff, Sorption processes in ion-exchange chromatography of viruses, J. Chromatogr. A 1142 (2007) 2–12.
[59] J. Kim, M.J. Park, M. Park, H.K. Shon, S.-H. Kim, J.H. Kim, Influence of colloidal fouling on pressure retarded osmosis, Desalination 389 (2016) 207–214.
[60] A. Zdziennicka, K. Szymczyk, B. Jańczuk, Correlation between surface free energy of quartz and its wettability by aqueous solutions of nonionic, anionic and cationic surfactants, J. Colloid Interface Sci. 340 (2) (2009) 243–248.
[61] S. Baliga, S. Muglikar, R. Kale, Salivary pH: A diagnostic biomarker, J. Indian Soc. Periodont. 17 (4) (2013) 461–465.
[62] L. Graetz, Ueber die Wärmeleitungsfähigkeit von Flüssigkeiten, Annalen der Physik 254 (79) (1882) 79–94.
[63] W.M. Deen, Analysis of Transport Phenomena, Oxford University Press, New York, Oxford, 1998.